

Synthesis and Biological Evaluation of 3-(1*H*-Imidazol- and Triazol-1-yl)-2,2-dimethyl-3-[4-(naphthalen-2-ylamino)phenyl]propyl Derivatives as Small Molecule Inhibitors of Retinoic Acid 4-Hydroxylase (CYP26)

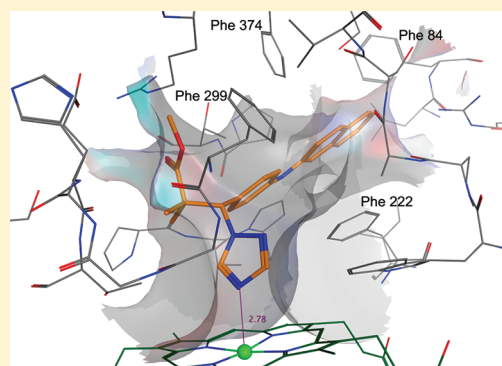
Mohamed S. Goma[†], Caroline E. Bridgens[‡], Gareth J. Veal[‡], Christopher P. F. Redfern[‡], Andrea Brancale[†], Jane L. Armstrong^{*,§} and Claire Simons^{*,†}

[†]Medicinal Chemistry Division, Welsh School of Pharmacy, Cardiff University, King Edward VII Avenue, Cardiff CF10 3NB, United Kingdom

[‡]Northern Institute for Cancer Research, Paul O'Gorman Building, Medical School, and [§]Institute of Cellular Medicine, Framlington Place, Newcastle University, Newcastle upon Tyne, NE2 4HH, United Kingdom

S Supporting Information

ABSTRACT: The synthesis and potent inhibitory activity of novel 3-(1*H*-imidazol- and triazol-1-yl)-2,2-dimethyl-3-[4-(naphthalen-2-ylamino)phenyl]propyl derivatives vs a MCF-7 CYP26A1 microsomal assay is described. This study focused on the effect of modifying the heme binding azole group and the flexible C3 chain on inhibitory activity and selectivity. The most promising inhibitor 2,2-dimethyl-3-[4-(naphthalen-2-ylamino)-phenyl]-3-[1,2,4]triazol-1-yl-propionic acid methyl ester (17) ($IC_{50} = 0.35$ nM as compared with liarozole $IC_{50} = 540$ nM and R116010 $IC_{50} = 10$ nM) was evaluated for CYP selectivity and hepatic stability. Compounds with CYP26 inhibitory IC_{50} values ≤ 50 nM enhanced the biological activity of exogenous ATRA, as evidenced by a 3.7–5.8-fold increase in CYP26A1 mRNA in SH-SY5Y neuroblastoma cells as compared with ATRA alone. All compounds demonstrated an activity comparable with or better than R116010, and the induction correlated well with CYP26 inhibition data. These studies highlight the promising activity profile of this novel CYP26 inhibitor and suggest it as an appropriate candidate for future development.



INTRODUCTION

Retinoic acid (RA) is a naturally occurring retinoid, the main biologically active derivative of vitamin A (retinol), which regulates cell growth and differentiation in a variety of cell types. As a key signaling molecule, the intracellular concentrations of RA are regulated by negative feedback controls tightly coupled to requirements for signaling in relation to cell differentiation and morphogenesis.^{1,2} Retinoids have long been major drugs used to treat disorders of keratinization such as acne, psoriasis, and ichthyosis^{3–6} and have been successful in the treatment of acute promyelocytic leukemia^{7,8} and neuroblastoma.⁹ Unfortunately, natural and induced resistance to RA as well as local and systemic toxicity limit the potential of RA in the treatment of these diseases and as a therapeutic strategy for a wider range of diseases.^{10,11}

One approach to overcoming drug resistance is to increase intracellular RA concentrations through inhibition of RA catabolic enzymes. The major enzyme responsible for RA metabolism is the RA-inducible cytochrome P450 (CYP) enzyme, CYP26.¹² CYP26 therefore provides a good target for the development of RA metabolism blocking agents (RAMBAs) to improve efficacy of retinoid treatment. Reducing the rate of metabolism of RA using

RAMBAs that can be cleared from the body on cessation of therapy may reduce the unwanted side effects associated with high-dose RA treatment.^{13,14}

Two RAMBAs have been developed clinically, the azoles liarozole and talarozole (Figure 1), both for dermatological treatment. In humans, topical application of liarozole exhibits similar clinical effects to the RA analogue acitretin but with fewer side effects.¹⁵ However, it lacks CYP26 specificity and inhibits steroidogenic CYP enzymes including aromatase (CYP19).¹⁶ In humans, talarozole (formerly R115866 and Rambazole) exhibits beneficial effects in both psoriasis¹⁷ and acne,¹⁸ and the side effects are expected to be less severe as compared with previous synthetic retinoids.¹⁹ *N*-(4-((1*R*,2*R*)-2-(Dimethylamino)-1-(1*H*-imidazol-1-yl)propyl)phenyl)-benzo[*d*]thiazol-2-amine (R116010)²⁰ (Figure 1) is a potent and selective inhibitor of RA metabolism, which inhibits all-*trans*-retinoic acid (ATRA) metabolism in neuroblastoma both in vitro and in vivo,²¹ although there are no further details regarding the clinical development of this RAMBA.

Received: June 1, 2011

Published: August 15, 2011

In previous studies,²² we reported the development of the lead CYP26 inhibitor, *N*-(4-((1*H*-imidazol-1-yl)(phenyl)methyl)phenyl)-naphthalen-2-amine (**1**) ($IC_{50} = 0.5 \mu\text{M}$; as compared with Liarozole, $IC_{50} = 540 \text{ nM}$, and R116010, $IC_{50} = 10 \text{ nM}$) by modification of the aryl, NH linker, and phenyl to a C3 chain (Figure 2).^{22,23} These studies indicated that a broad range of aryl and heteroaryl substituents were tolerated, that the NH linker was optimal with a noted reduction in inhibitory activity if replaced with either an $-\text{O}-$ or a $-\text{CH}_2-$ linker, and that the dimethyl group was important in establishing hydrophobic interactions and optimizing “fit” within the CYP26 active site. Several low nanomolar inhibitors were discovered through structure–activity relationship (SAR) studies with methyl 3-(1*H*-imidazol-1-yl)-2,2-dimethyl-3-(4-(naphthalen-2-ylamino)phenyl)propanoate (**2**) ($IC_{50} = 3 \text{ nM}$, Figure 2) evaluated further for selectivity and hepatic stability. Direct comparison of CYP selectivity profiles for compound **2** and R116010 revealed markedly reduced activity as compared with CYP26 for CYPs 1A2, 2C9, 2C19, and 2D6. However, both compounds exhibited activity against CYP3A4, a xenobiotic-metabolizing CYP with low substrate specificity and which is known to have activity as an ATRA hydroxylase, with IC_{50} values of $<0.1 \mu\text{M}$ for compound **2** and $0.35 \mu\text{M}$ for R116010.

CYP3A4 liability will restrict further development of RAMBAs for systemic use, although likely to be less of an issue for topical administration in combination with ATRA; therefore, further SAR studies were required to determine the effect on selectivity and inhibitory activity. The two areas for SAR studies described here are the C3 flexible chain and the heme binding azole (Figure 2).

RESULTS

Chemistry. The synthesis of several ester and amide analogues of (**2**) was undertaken. The preparation of the acid (**4**) was performed through saponification of the lead compound (**2**) with KOH in EtOH under reflux.²⁴ The acid was separated in good yield after acidification of the potassium salt (**3**) with aqueous 1 N HCl followed by extraction with dichloromethane (Scheme 1).

Several esters (**5–9**) were prepared by stirring the potassium salt (**3**) with the corresponding alkyl halides in EtOH at room

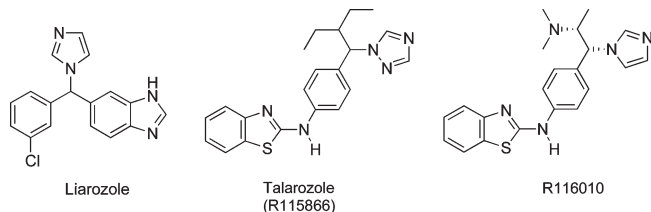


Figure 1. RAMBAs.

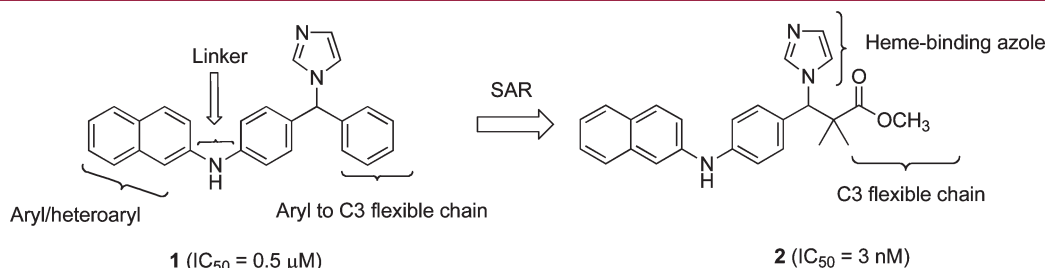


Figure 2. Development of compounds through SAR studies.

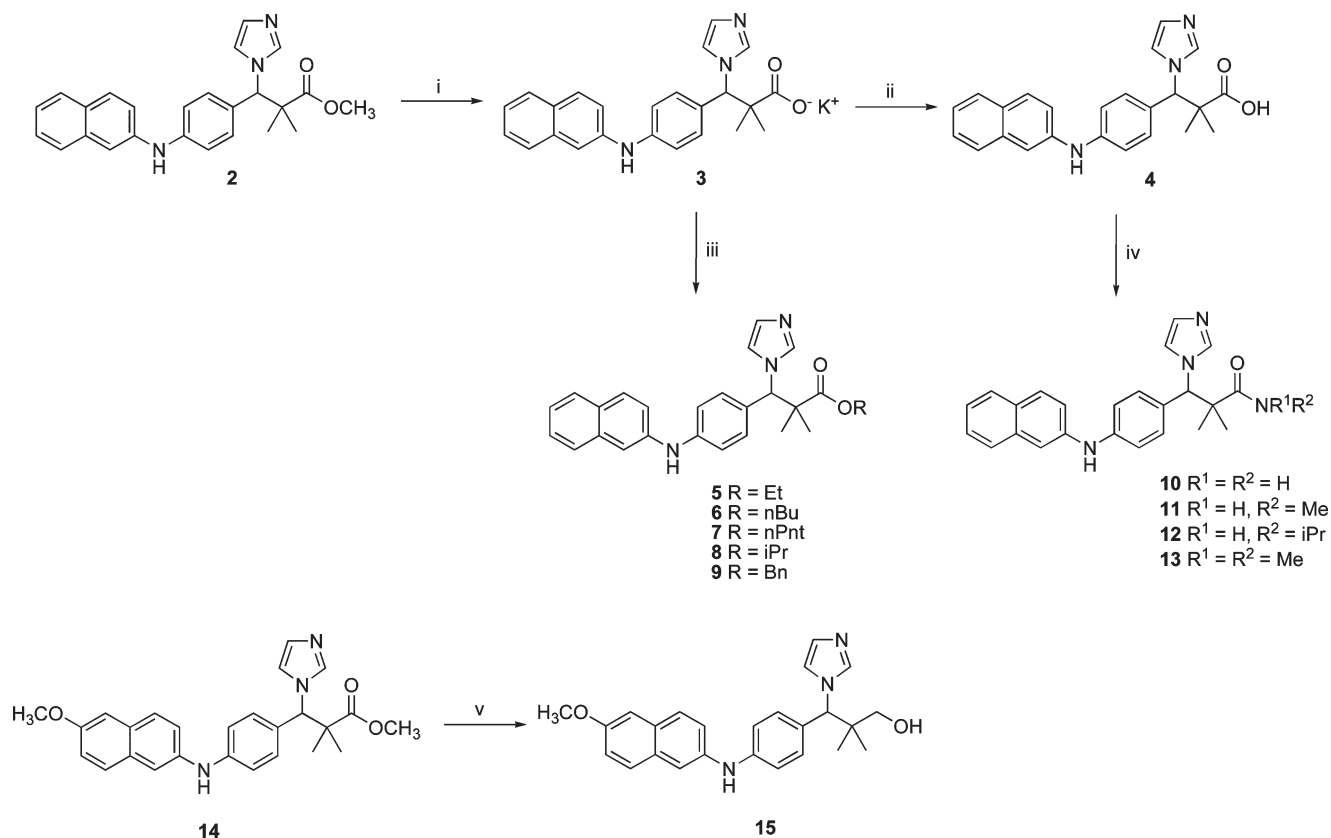
temperature, with the ester products obtained in good yield after purification by column chromatography (Scheme 1). The amide derivatives (**10–13**) were prepared through the reaction of the acid (**4**) with an amine in the presence of EDC and HOBT in dichloromethane^{25,26} and obtained in good yield after purification by flash column chromatography. The alcohol analogue (**15**) of compound (**14**)²² was generated by reduction with LiAlH_4 in THF²⁷ (Scheme 1).

The modification of the *N*-heterocycle moiety involved the preparation of triazole derivatives. The triazole analogue was prepared through the reaction of the alcohol precursor (**16**)²² with 1,1'-carbonylditriazole and triazole in acetonitrile to give the triazole derivative (**17**) in good yield (63%) (Scheme 2). Attempts to prepare the triazole acid (**18**) derivative following the previously described method for the imidazole acid (**4**) using KOH and EtOH were unsuccessful with no reaction observed; however, hydrolysis of the triazole ester (**17**) was accomplished with LiOH in THF and H_2O .^{26,28} The acid was obtained in good yield after acidification (pH 3) and extraction with diethyl ether and used without further purification. The triazole amide derivative (**19**) was obtained after treatment of the acid (**18**) with methylamine in the presence of EDC and HOBT in dichloromethane (Scheme 2).^{25,26}

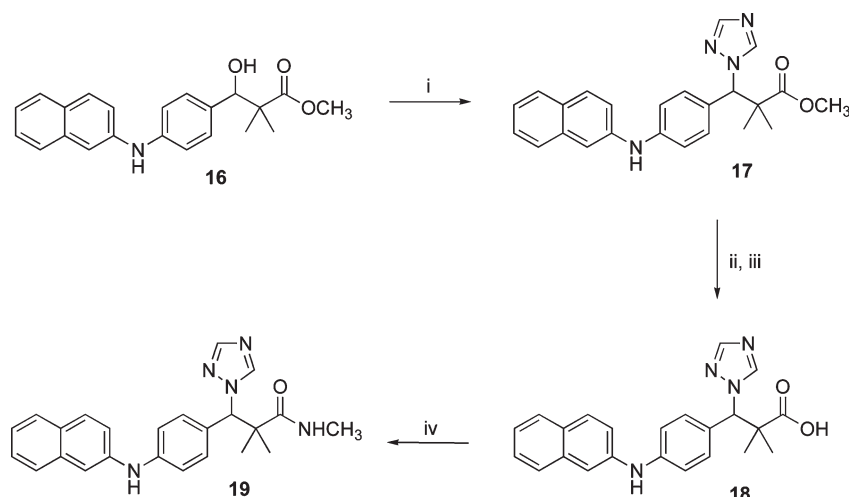
Enzyme Inhibition. The imidazole and triazole derivatives were evaluated for their RA metabolism (CYP26) inhibitory activity with a cell-free microsomal assay,^{23,29} using radiolabeled $[11,12\text{-}^3\text{H}]\text{ATRA}$ as the substrate. Liarozole (a nonselective CYP26 inhibitor^{15,16}) and R116010²⁰ were included in all experiments as comparative standards.

In the ester series (**2** and **5–9**), a small alkyl substituent was optimal with the methyl ester (**2**, $IC_{50} = 3 \text{ nM}$) and ethyl ester (**5**, $IC_{50} = 0.35 \text{ nM}$) being preferred as compared with larger chains such as butyl (**6**) and pentyl (**7**) ($IC_{50} = 200$ and 140 nM , respectively), branched isopropyl (**8**, $IC_{50} = 290 \text{ nM}$), and the bulky aromatic benzyl ester (**9**, $IC_{50} = 400 \text{ nM}$) (Table 1). It is probable that the enhanced inhibitory activity observed for the ethyl ester (**5**) is related to pharmacodynamic properties rather than enhanced binding, whereas for the larger alkyl esters a reduced fit has a direct impact on inhibitory activity. Replacing the ester with an amide (**10–13**) was generally well tolerated (IC_{50} range = $12\text{--}120 \text{ nM}$) with the methyl amide isostere (**11**) of the lead methyl ester (**2**) displaying comparable inhibitory activity with an IC_{50} of 12 nM . The order of preference for inhibitory activity of the amides was $\text{NHMe} > \text{NH}_2 > \text{NMe}_2 > \text{NH}^i\text{Pr}$. Removal of the alkyl group to give the free carboxylic acid (**4**) resulted in a reduction in activity from 3 to 300 nM , whereas reduction of the ester to the free alcohol (**15**) was tolerated ($IC_{50} = 40 \text{ nM}$).

The triazole methyl ester (**17**) showed improved subnanomolar inhibitory activity ($IC_{50} = 0.35 \text{ nM}$) as compared with the imidazole methyl ester lead (**2**, $IC_{50} = 3 \text{ nM}$) (Table 2).

Scheme 1^a

^a Reagents and conditions: (i) KOH, EtOH, reflux, 72 h. (ii) 1 N aqueous HCl, 64%. (iii) RBr, DMF, 80 °C, 2 h, 57–71%. (iv) EDC, HOBT, CH₂Cl₂, 0.5 h, room temperature and then R¹R²NH, room temperature, overnight, 61–75%. (v) LiAlH₄, THF, 0 °C, 1 h and then room temperature overnight, 79%.

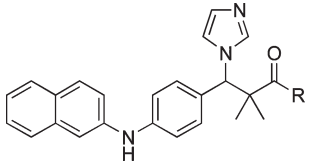
Scheme 2^a

^a Reagents and conditions: (i) 1,1'-Carbonylditriazole, triazole, CH₃CN, reflux, 16 h, 63%. (ii) LiOH, THF, H₂O, 20 h, reflux and then (iii) aqueous 1 N HCl 77%. (iv) EDC, HOBT, CH₂Cl₂, 0.5 h, room temperature and then CH₃NH₂, room temperature, overnight, 63%.

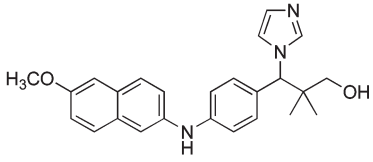
However, a considerable reduction in activity was noted for the triazole carboxylic acid derivative (**18**, IC₅₀ > 1 μM) as compared with the imidazole carboxylic acid derivative (**4**, IC₅₀ = 300 nM), and this same trend was observed for the triazole methyl amide

derivative (**19**, IC₅₀ = 350 nM) as compared with imidazole product (**11**, IC₅₀ = 12 nM) (Table 2).

Enhancement of RA Effects. The induction of CYP26A1 mRNA was used to determine the ability of the compounds to

Table 1. IC₅₀ Values for Imidazole Esters, Amides, and Alcohol


Compd	R	CYP26 IC ₅₀ (nM) ^a
2	OCH ₃	3
4	OH	300
5	OCH ₂ CH ₃	0.35
6	O(CH ₂) ₃ CH ₃	200
7	O(CH ₂) ₄ CH ₃	140
8	OCH(CH ₃) ₂	290
9	OCH ₂ Ph	400
10	NH ₂	50
11	NHCH ₃	12
12	NHCH(CH ₃) ₂	120
13	N(CH ₃) ₂	75
15		40



Liarozole	-	540
R116010	-	10

^aIC₅₀ values were derived from the best fit of a four point dose–response curve.

Table 2. IC₅₀ Values for Triazole Compounds as Compared with Imidazole Compounds

Triazole			Imidazole		
no.	R	CYP26 IC ₅₀ (nM) ^a	no.	R	CYP26 IC ₅₀ (nM) ^a
17	OCH ₃	0.35	2	OCH ₃	3
18	OH	>1 μM	4	OH	300
19	NHCH ₃	350	11	NHCH ₃	12

^aIC₅₀ values were derived from the best fit of a 4 point dose–response curve. Liarozole, IC₅₀ = 540 nM; R116010, IC₅₀ = 10 nM.

enhance the biological effects of ATRA in retinoid-responsive SH-SY5Y neuroblastoma cells. Compounds with a microsomal

CYP26 inhibitory IC₅₀ ≤ 50 nM were selected, and CYP26A1 mRNA was not induced by treatment of SH-SY5Y cells with these inhibitors alone at a concentration of 1 μM. Coincubation of liarozole with 0.1 μM ATRA resulted in a 2.3-fold induction in CYP26A1 mRNA as compared with 0.1 μM ATRA alone, whereas coincubation with R116010 resulted in a 4.7-fold induction of CYP26A1 mRNA, which was comparable to the induction in response to a 10-fold higher concentration of ATRA (1 μM) (Figure 3). Coincubation of 0.1 μM ATRA in combination with 1 μM compounds **2**, **5**, **10**, **11**, **15**, and **17** for 72 h also substantially increased expression of CYP26A1 as compared with 0.1 μM ATRA alone. Under these conditions, the two compounds with the greatest CYP26 inhibitory activity, the ethyl ester product **5** and the triazole methyl ester **17**, enhanced the expression of CYP26A1 mRNA by 5.8- and 5.2-fold, respectively (Figure 3). Conversely, the two compounds with the lowest CYP26 inhibitory activity, the reduced ester **15** and the amide **10**, enhanced CYP26A1 mRNA by 3.7- and 4.1-fold, respectively, and were the least active (Figure 3).

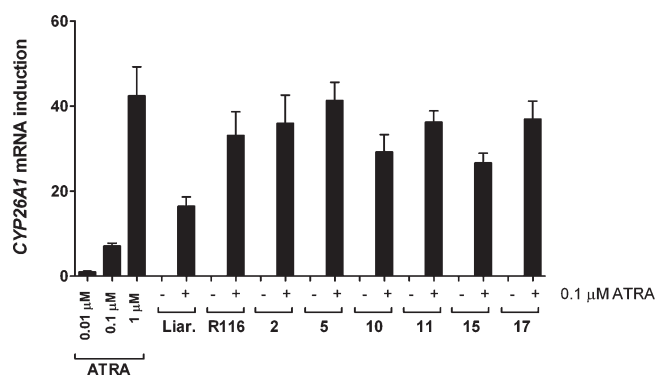


Figure 3. Real-time PCR analysis of CYP26A1 mRNA expression after treatment with ATRA in combination with liarozole (Liar.), R116010 (R116), 2, 5, 10, 11, 15, and 17. SH-SY5Y cells were treated with ATRA alone (0.01–1 μM) or with ATRA (0.1 μM) in combination with inhibitor (1 μM) for 72 h. Total RNA was isolated, reverse transcribed, and subjected to real-time PCR using TaqMan probes for CYP26A1 and β -actin. Values were normalized for β -actin levels and expressed as a fold increase relative to CYP26A1 expression in SH-SY5Y cells treated with 0.01 μM ATRA. Data are mean values \pm SDs ($n = 6$).

Table 3. Percent Inhibition Data against CYP Panel at 0.4 μM

Compound	1A2	3A4	2C9	2C19	2D6
2	21	60	41	11	25
5	20	61	43	30	15
11	15	86	45	14	13
13	11	95	52	21	29
17	10	22	38	16	-2

Inactive Border line Highly active

Selectivity and Microsomal Stability. The imidazole ethyl ester (5), imidazole methylamide (11), imidazole dimethylamide (13), and triazole methyl ester (17) derivatives were evaluated for their inhibitory activity against a panel of P450 isoforms expressed in human liver microsomes (Table 3) in comparison with the lead imidazole methyl ester (2). The imidazole ethyl ester (5) had a CYP selectivity profile almost identical with the methyl ester lead (2). The amides 11 and 13 were highly active against CYP3A4 at concentrations of 0.4 μM , which would discount these compounds for further evaluation. However, at this concentration, the triazole methyl ester (17) was inactive against the CYP panel (Table 3).

To determine the selectivity of the triazole methyl ester (17) in comparison with R116010 and the lead imidazole methyl ester (2), IC_{50} assays against CYP isoforms expressed in human liver microsomes were performed. Micromolar concentrations of compounds 2 or 17 or R116010 were needed to inhibit CYPs 1A2, 2C9, and 2C19.

Furthermore, compound 17 was ≥ 6000 -fold more potent against CYP26 as compared to CYPs 1A2, 2C9, 2C19, and 2D6, with compound 2 and R116010 ≥ 200 - and ≥ 400 -fold more potent, respectively. However, although all three compounds inhibited CYP3A4 with submicromolar activity, an improvement was observed with the triazole methyl ester (17) showing reduced potency against CYP3A4 ($\text{IC}_{50} = 0.33 \mu\text{M}$) as compared

Table 4. CYP IC_{50} (μM) Profile of Triazole 17 as Compared with Lead 2 and R116010

compd	1A2	2C9	2C19	3A4	2D6	26
17	10.9	21.4	3.14	0.33	1.8	0.0003
2	1.2	8.0	1.5	<0.1	0.6	0.003
R116010	8.3	11.0	5.9	0.35	3.9	0.01

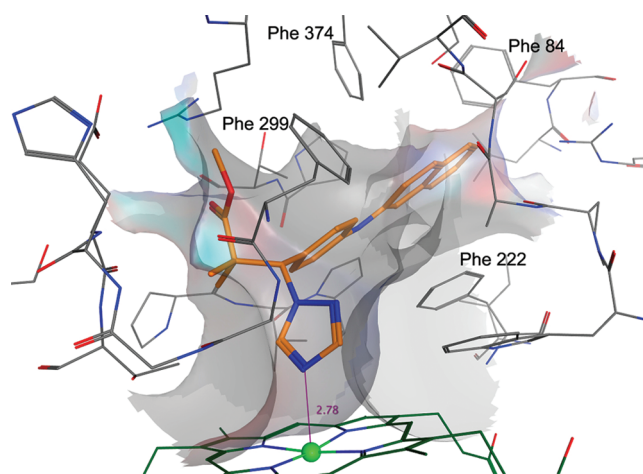


Figure 4. Putative binding mode for 17. The Fe atom of the heme is shown as a green sphere.

with imidazole (2), which was comparable with R116010 (CYP3A4 $\text{IC}_{50} = 0.35 \mu\text{M}$) (Table 4). Compound 17 exhibited a low clearance rate (Cyprotex: $t_{1/2} = 3$ h and 44 min) in human liver microsomes comparable with the imidazole lead 2 (Cyprotex: $t_{1/2} = 5$ h and 1 min), indicating minimal phase I metabolism and good stability.³⁰

Molecular Modeling. A series of molecular docking simulations were performed on this series of compounds with ligands docked within the active site of the CYP26A1 homology model,³¹ following the methodology reported previously.²² Results obtained for 17 showed a putative binding mode very similar to the one observed previously with the corresponding imidazole analogue 2.²² In particular, the binding was dominated by a series of hydrophobic interactions: The naphthyl group lay in a channel formed, among others, by Phe222, Phe84, and Phe374, while the ester moiety was in contact with Phe299 (Figure 4). The naphthylphenylamine moiety is not common in drugs; however, in these inhibitors, it fulfills the role of binding the molecule in the hydrophobic tunnel of the enzyme active site and allows correct orientation of the imidazole for optimal interaction with the heme.

DISCUSSION

Evaluation of CYP26 inhibitory activity revealed that in the imidazole ester series, 2 and 5–9, a small alkyl group was optimal with the methyl (2) and ethyl (5) esters displaying potent inhibitory activity (2, $\text{IC}_{50} = 3$ nM; 5, $\text{IC}_{50} = 0.35$ nM) as compared with the longer and branched chain esters and bulky aromatic ester groups (6–9, IC_{50} range = 140–400 nM). A similar pattern was observed in the amide imidazole series with the methyl amide –CONHMe (11) showing optimal activity ($\text{IC}_{50} = 12$ nM) as compared with the dimethyl amide (13) and

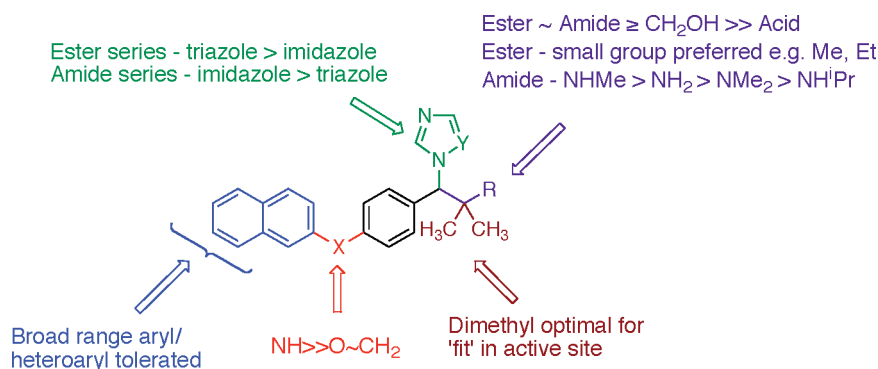


Figure 5. Optimal SAR for the 2,2-dimethyl-3-(4-(naphthalen-2-ylamino)phenyl) propyl azole derivatives.

branched isopropyl amide (**12**). These data would suggest that one H-bond donor and a small alkyl group are preferred for activity in the amide series. Although the esters (**6–9**) and amides (**10, 12**, and **13**) were less active than the lead compound (**2**), they were more active than liarozole ($IC_{50} = 540$ nM). The 2,2-dimethyl-3-propanol derivative (**15**) also showed good inhibitory activity ($IC_{50} = 40$ nM), suggesting that a carbonyl group is not essential for activity.

The triazole equivalents of the most potent compounds in the imidazole series, the methyl ester (**2**) and methyl amide (**11**), were prepared for evaluation. The triazole methyl ester (**17**) was more potent with an IC_{50} of 0.35 nM, while the triazole methyl amide (**19**) showed a reduction in activity with an IC_{50} of 350 nM as compared with the corresponding imidazole derivatives. The triazole carboxylic acid derivative (**18**) showed a loss in activity ($IC_{50} > 1$ μ M) as compared with the imidazole carboxylic acid (**4**, $IC_{50} = 350$ nM); this loss in activity may be related to reduced uptake; however, the metabolic stability of the ester, assessed previously,²² would suggest that the ester is the active inhibitor rather than acting as a prodrug for the carboxylic acid.

Compounds with biochemical CYP26 inhibitory IC_{50} values ≤ 50 nM also enhanced the biological activity of exogenous ATRA, as evidenced by a 3.7–5.8-fold increase in CYP26A1 induction as compared to ATRA alone. All compounds demonstrated an activity comparable with or better than R116010, and the induction correlated well with CYP26 inhibition data. Direct comparison of CYP selectivity profiles for triazole **17** and R116010 revealed an almost identical CYP selectivity profile; however, the greater CYP26 inhibitory activity of **17** as compared with R116010 resulted in compound **17** being ≥ 6000 -fold more potent against CYP26 as compared with CYPs 1A2, 2C9, 2C19, and 2D6, with R116010 ≥ 400 -fold more potent, respectively. Importantly, the triazole (**17**) displayed improved CYP3A4 selectivity (1100-fold more selective for CYP26) as compared with the imidazole (**2**) (<33-fold more selective for CYP26).

The studies have allowed evaluation of SAR with key functional groups and optimal interactions noted (Figure 5), with the promising biological activity profile of the triazole ester **17**, suggesting that it is an appropriate candidate for further evaluation and development for use in the treatment of dermatological diseases.

EXPERIMENTAL SECTION

General Procedures. [¹¹,¹²-³H]-All *trans*-retinoic acid (37 MBq/mL) and Ultima Flo M scintillation fluid were purchased from Perkin-Elmer

(United Kingdom). Acetic acid and ammonium acetate were obtained from Fisher Scientific (United Kingdom). All solvents used for chromatography were high-performance liquid chromatography (HPLC) grade from Fisher Scientific.

¹H and ¹³C NMR spectra were recorded with a Bruker Avance DPX500 spectrometer operating at 500 and 125 MHz, with Me₄Si as an internal standard. Mass spectra were determined by the EPSRC mass spectrometry center (Swansea, United Kingdom). Microanalyses were determined by Medac Ltd. (Surrey, United Kingdom). CYP26 selectivity assays were performed by Cyprotex (Cheshire, United Kingdom). Flash column chromatography was performed with silica gel 60 (230–400 mesh) (Merck), and thin-layer chromatography (TLC) was carried out on precoated silica plates (kiesel gel 60 F₂₅₄, BDH). Compounds were visualized by illumination under UV light (254 nm). Melting points were determined on an electrothermal instrument and are uncorrected. All solvents were dried prior to use as described by the handbook Purification of Laboratory Chemicals³² and stored over 4 Å molecular sieves, under nitrogen. All compounds were more than 95% pure.

Cell Culture and Retinoid Treatment. SH-SY5Y or MCF-7 cells were cultured at 37 °C in RPMI 1640 medium containing fetal calf serum (10%) and L-glutamine (2 mM) in a humidified atmosphere of 5% CO₂ in air. ATRA was dissolved in dimethyl sulfoxide and added to the culture medium as described by Armstrong et al.²¹ Liarozole, R116010, and imidazole/triazole derivatives were dissolved in ethanol and diluted in cell culture medium. The final concentration of ethanol in all experiments never exceeded 0.8%.

Microsomal CYP26 Inhibition Assay. MCF-7 cells were pre-treated for 24 h with 1 μ M ATRA to induce CYP26 expression. Microsomes were prepared as described by Han and Choi.²⁹ Briefly, cells were homogenized in buffer A [10 mM Tris, pH 7.4, 1 mM EDTA, 0.5 M sucrose, and Complete Protease Inhibitor Cocktail (Roche, United Kingdom)] using a Dounce homogenizer, diluted with an equal volume of Tris/EDTA, and the diluted homogenate laid over a volume of buffer A equal to the original volume. Microsomes were then isolated by differential centrifugation (9000g, 10 min, 4 °C; 100000g, 60 min, 4 °C). The microsomal pellet was suspended in buffer B (10 mM Tris, pH 7.4, 1 mM EDTA, 0.25 M sucrose, and Complete Protease Inhibitor Cocktail) and stored at –70 °C. Cytochrome *c* reductase activity was calculated at 5–15 U cyt *c*/μg protein, using the cytochrome *c* reductase (NADPH) kit (Sigma) according to the manufacturer's instructions. For ATRA metabolism, 50 μg of microsomal protein was incubated in assay buffer (50 mM Tris, pH 7.4, 150 mM KCl, 10 mM MgCl₂, 0.02% w/v BSA, 2 mM NADPH, 10 nM ATRA, and 0.1 μCi ³H-ATRA) in amber eppendorfs in the absence or presence of CYP26 inhibitor (1–1000 nM) in a final volume of 200 μL for 1 h at 37 °C with shaking. The reaction was quenched with acetonitrile, mixed, and then centrifuged (18000g, 5 min, 4 °C). Resolution of retinoids was performed with a Luna C18(2) column (3 μm, 50 mm × 2 mm) using a Waters

2690 Separations Module and subsequent Radiomatic Series 500TR Flow Scintillation Analyzer (Packard Biosciences), with Empower 2 Chromatography Data Software and Flow-ONE software, respectively, for data acquisition. ^3H -ATRA and ^3H metabolites were separated by gradient reversed-phase chromatography, using mobile phase A [50% acetonitrile, 50% (0.2%) acetic acid, w/w] and mobile phase B (acetonitrile, 0.1% acetic acid, w/w). A flow rate of 0.3 mL/min was used with linear gradients employed between the specified times as follows: 0, 100% A; 5 min, 100% A; 5.5 min, 40% A, 60% B; 12 min, 40% A, 60% B; 12.5 min, 20% A, 80% B; 17.5 min, 20% A, 80% B; 18 min, 100% A; 25 min, 100% A. The scintillant flow rate was 1 mL/min. CYP26 inhibition was calculated as the percentage ^3H ATRA metabolite peak area formation (activity ^3H metabolite(s)/total activity) as compared to metabolite formation in the absence of inhibitor. IC_{50} values were calculated by nonlinear regression analysis in SigmaPlot (Systat Software Inc., United States) using an inhibition curve constructed from a minimum of four data points. Compound 2 was used as a standard in every assay.

Real-Time Polymerase Chain Reaction (PCR) for CYP26A1 Expression. RNA was isolated using an RNeasy Kit (Qiagen, Crawley, United Kingdom), reverse-transcribed and real-time PCR performed on 20 ng of cDNA using TaqMan Gene Expression products for human CYP26A1 in combination with the TaqMan Universal PCR master mix (Applied Biosystems, Warrington, United Kingdom) on a GeneAmp 5700 Sequence Detection System as described previously.²¹

Chemistry. General Method—Synthesis of the Esters (5–9). Methyl 3-(1*H*-imidazol-1-yl)-2,2-dimethyl-3-[4-(naphthalen-2-ylamino)phenyl]propanoate (**2**)²² (2.0 mmol) in EtOH (20 mL) was saponified with KOH (4.0 mmol) under reflux for 72 h. The solvent was removed under reduced pressure, then H_2O (100 mL) was added, and the unreacted starting materials were extracted with diethyl ether (3 × 50 mL). The H_2O layer was reduced in vacuo to give the potassium salt (**3**), which was dissolved in anhydrous DMF. Alkylbromide (2.4 mmol) was added, and the mixture was heated at 80 °C for 2 h. H_2O (70 mL) was then added, and the aqueous layer was extracted with EtOAc (3 × 50 mL). The organic layer was dried (MgSO_4), filtered, and reduced in vacuo. The product was purified by flash column chromatography (CH_2Cl_2 –MeOH 100:0 v/v increasing to 97:3 v/v).

Ethyl 3-(1*H*-imidazol-1-yl)-2,2-dimethyl-3-[4-(naphthalen-2-ylamino)phenyl]propanoate (**5**). Compound **5** was prepared from reaction of (**2**) and ethylbromide in 71% yield as a white solid; mp 156–158 °C. TLC (97:3 CH_2Cl_2 /MeOH, R_f = 0.62). ^1H NMR (CDCl_3): δ 1.21 (t, J = 7.0 Hz, 3H, CH_2CH_3), 1.37 (s, 6H, H-3, H-4), 4.13 (q, J = 7.0 Hz, 1H, CH_2CH_3), 5.58 (s, 1H, H-5), 6.11 (s, 1H, NH), 7.08 (m, 3H, Ar), 7.19 (m, 2H, Ar), 7.25 (m, 2H, Ar), 7.31 (s, 1H, imid), 7.35 (m, 1H, Ar), 7.41 (m, 1H, Ar), 7.49 (d, J = 8.2 Hz, 1H, Ar), 7.77 (m, 1H, Ar), 7.85 (m, 2H, Ar). EI-HRMS ($M + \text{H}$)⁺ found, 414.2179; calcd for $\text{C}_{26}\text{H}_{27}\text{N}_3\text{O}_2$, 414.2181.

Butyl 3-(1*H*-imidazol-1-yl)-2,2-dimethyl-3-[4-(naphthalen-2-ylamino)phenyl]propanoate (**6**). Compound **6** was prepared from reaction of (**2**) and butylbromide in 67% yield as a yellow oil. TLC (97:3 CH_2Cl_2 /MeOH, R_f = 0.65). ^1H NMR (CDCl_3): δ 0.96 (t, J = 6.9 Hz, 3H, butyl), 1.23 (m, 8H, CH_2 -butyl, H-3, H-4), 1.48 (m, 2H, butyl), 4.12 (t, J = 6.6 Hz, 2H, butyl), 5.08 (s, 1H, H-7), 5.93 (s, 1H, NH), 7.15 (d, J = 8.0 Hz, 2H, Ar), 7.22 (m, 2H, Ar), 7.41 (m, 3H, Ar), 7.50 (s, 1H, imid), 7.52 (s, 1H, imid), 7.74 (d, J = 8.2 Hz, 2H, Ar), 7.82 (m, 3H, Ar). EI-HRMS ($M + \text{H}$)⁺ found, 442.2483; calcd for $\text{C}_{28}\text{H}_{31}\text{N}_3\text{O}_2$, 442.2489.

Pentyl 3-(1*H*-imidazol-1-yl)-2,2-dimethyl-3-[4-(naphthalen-2-ylamino)phenyl]propanoate (**7**). Compound **7** was prepared from reaction of (**2**) and pentylbromide in 69% yield as a yellow oil. TLC (97:3 CH_2Cl_2 /MeOH, R_f = 0.65). ^1H NMR (CDCl_3): δ 0.95 (t, J = 6.8 Hz, 3H, pentyl), 1.25 (m, 10H, 2 × CH_2 pentyl, H-3, H-4), 1.52 (m, 2H, pentyl), 4.08 (t, J = 6.5 Hz, 2H, pentyl), 5.55 (s, 1H, H-5), 6.01 (s, 1H, NH), 7.19 (m, 4H, Ar), 7.33 (m, 3H, Ar), 7.42 (m, 1H, Ar), 7.48 (m, 2H, Ar), 7.74 (m, 2H,

Ar), 7.82 (m, 2H, Ar). EI-HRMS ($M + \text{H}$)⁺ found, 456.2637; calcd for $\text{C}_{29}\text{H}_{33}\text{N}_3\text{O}_2$, 456.2632.

Isopropyl 3-(1*H*-imidazol-1-yl)-2,2-dimethyl-3-[4-(naphthalen-2-ylamino)phenyl]propanoate (**8**). Compound **8** was prepared from reaction of (**2**) and isopropylbromide in 68% yield as a white solid; mp 166–168 °C. TLC (97:3 CH_2Cl_2 /MeOH, R_f = 0.65). ^1H NMR (CDCl_3): δ 1.11 (d, J = 6.8 Hz, 6H, ^iPr), 1.29 (s, 6H, H-3, H-4), 4.93 (sep, J = 6.8 Hz, 1H, ^iPr), 5.54 (s, 1H, H-5), 6.13 (s, 1H, NH), 7.07 (d, J = 8.1 Hz, 2H, Ar), 7.19 (m, 2H, Ar), 7.27 (m, 2H, Ar), 7.31 (s, 1H, imid), 7.39 (m, 1H, Ar), 7.50 (m, 2H, Ar), 7.68 (d, J = 8.2 Hz, 2H, Ar), 7.76 (d, J = 8.3 Hz, 2H, Ar). EI-HRMS (M)⁺ found, 428.2337; calcd for $\text{C}_{27}\text{H}_{29}\text{N}_3\text{O}_2$, 428.2338.

Benzyl 3-(1*H*-imidazol-1-yl)-2,2-dimethyl-3-[4-(naphthalen-2-ylamino)phenyl]propanoate (**9**). Compound **9** was prepared from reaction of (**2**) and benzylbromide in 57% yield as a yellow oil. TLC (97:3 CH_2Cl_2 /MeOH, R_f = 0.65). ^1H NMR (CDCl_3): δ 1.25 (s, 6H, H-3, H-4), 5.06 (s, 2H, benzyl), 5.55 (s, 1H, H-5), 5.94 (s, 1H, NH), 7.08 (d, J = 8.0 Hz, 2H, Ar), 7.15 (d, J = 7.8 Hz, 2H, Ar), 7.21 (m, 4H, Ar), 7.36 (m, 5H, Ar), 7.47 (m, 3H, Ar), 7.66 (d, J = 8.1 Hz, 1H, Ar), 7.71 (m, 2H, Ar). EI-HRMS ($M + \text{H}$)⁺ found, 476.2323; calcd for $\text{C}_{31}\text{H}_{29}\text{N}_3\text{O}_2$, 476.2319.

3-(1*H*-imidazol-1-yl)-2,2-dimethyl-3-[4-(naphthalen-2-ylamino)phenyl]propanoic Acid (**4**). Methyl 3-(1*H*-imidazol-1-yl)-2,2-dimethyl-3-[4-(naphthalen-2-ylamino)phenyl]propanoate (**2**)²² (2.0 mmol) in EtOH (20 mL) was saponified with KOH (4.0 mmol) under reflux for 72 h. The solvent was removed under reduced pressure, H_2O (100 mL) was added, and the unreacted starting materials were extracted with ether (3 × 50 mL). The H_2O layer was acidified with 1 N aqueous HCl until pH 3 and extracted with CH_2Cl_2 (100 mL). The organic layer was dried (MgSO_4), and the solvent was removed under reduced pressure to give the product in 64% yield as a brown solid; mp 148–150 °C. TLC (97:3 CH_2Cl_2 /MeOH, R_f = 0.21). ^1H NMR (CDCl_3): δ 1.25 (s, 3H, H-3), 1.33 (s, 3H, H-4), 5.67 (s, 1H, H-NH), 7.07 (d, J = 8.0 Hz, 2H, Ar), 7.11 (s, 1H, H-5), 7.17 (s, 1H, Ar), 7.25 (m, 2H, Ar), 7.32 (m, 3H, Ar), 7.47 (s, 1H, imid), 7.50 (s, 1H, imid), 7.71 (d, J = 8.2 Hz, 1H, Ar), 7.83 (s, 1H, imid), 7.77 (m, 2H, Ar), 8.23 (s, 1H, CO_2H). EI-HRMS ($M + \text{H}$)⁺ found, 386.1865; calcd for $\text{C}_{24}\text{H}_{23}\text{N}_3\text{O}_2$, 386.1863.

General Method—Synthesis of the Amides. EDC (0.18 mmol), carboxylic acid (**4** or **18**) (0.18 mmol), and HOBt (0.18 mmol) in CH_2Cl_2 (10 mL) were stirred at room temperature under N_2 for 0.5 h. Amine (0.56 mmol) was added, and the reaction mixture was stirred overnight. EtOAc (70 mL) was added, and the organic layer was washed with 1 M aqueous HCl (30 mL), saturated aqueous NaHCO_3 (30 mL), brine (30 mL), and H_2O (30 mL). The organic layer was dried (MgSO_4), filtered, and reduced in vacuo. The residue was purified by flash column chromatography (CH_2Cl_2 –MeOH 100:0 v/v increasing to 98:2 v/v).

3-(1*H*-imidazol-1-yl)-2,2-dimethyl-3-[4-(naphthalen-2-ylamino)phenyl]propanamide (**10**). Compound **10** was prepared from reaction of (**4**) and methanolic NH_3 in 71% yield as a brown oil. TLC (97:3 CH_2Cl_2 /MeOH, R_f = 0.47). ^1H NMR (CDCl_3): δ 1.27 (s, 3H, H-3), 1.29 (s, 3H, H-4), 5.53 (s, 1H, H-5), 5.59 (s, 2H, NH_2), 5.89 (s, 1H, NH), 7.05 (d, J = 8.2 Hz, 2H, Ar), 7.17 (s, 1H, imid), 7.22 (m, 4H, Ar), 7.29 (m, 1H, Ar), 7.35 (m, 1H, Ar), 7.46 (s, 1H, imid), 7.63 (d, J = 8.0 Hz, 1H, Ar), 7.73 (d, J = 8.1 Hz, 2H, Ar), 7.81 (s, 1H, imid). EI-HRMS ($M + \text{H}$)⁺ found, 385.2026; calcd for $\text{C}_{24}\text{H}_{24}\text{N}_4\text{O}$, 385.2028.

3-(1*H*-imidazol-1-yl)-*N*,2,2-trimethyl-3-[4-(naphthalen-2-ylamino)phenyl]propanamide (**11**). Compound **11** was prepared from reaction of (**4**) and 33% methylamine in absolute EtOH in 75% yield as a brown solid; mp 120–124 °C. TLC (97:3 CH_2Cl_2 /MeOH, R_f = 0.50). ^1H NMR (CDCl_3): δ 1.26 (s, 3H, H-3), 1.29 (s, 3H, H-4), 2.75 (d, J = 2.5 Hz, 3H, NHCH_3), 5.62 (s, 1H, H-5), 5.77 (d, J = 2.5 Hz, 1H, NHCH_3), 6.11 (s, 1H, NH), 7.04 (s, 1H, imid), 7.09 (d, J = 8.2 Hz, 1H, Ar), 7.15 (s, 1H, imid), 7.22 (m, 4H, Ar), 7.30 (m, 1H, Ar), 7.39 (m, 1H,

Ar), 7.45 (d, $J = 2.6$ Hz, 1H, Ar), 7.65 (m, 2H, Ar), 7.76 (d, $J = 8.1$ Hz, 2H, Ar). Anal. C, H, N.

3-(1*H*-imidazol-1-yl)-*N*-isopropyl-2,2-dimethyl-3-[4-(naphthalen-2-ylamino)phenyl]propanamide (**12**). Compound **12** was prepared from reaction of (**4**) and isopropylamine in 64% yield as a pale yellow oil. TLC (97:3 CH₂Cl₂/MeOH, $R_f = 0.56$). ¹H NMR (CDCl₃): δ 1.08 (d, $J = 6.6$ Hz, 6H, NHⁱPr), 1.25 (s, 3H, H-3), 1.29 (s, 3H, H-4), 4.13 (sep, $J = 6.6$ Hz, 1H, NHⁱPr), 5.41 (d, $J = 6.6$ Hz, 1H, NHⁱPr), 5.63 (s, 1H, NH), 6.16 (s, 1H, H-5), 7.08 (m, 3H, Ar), 7.23 (m, 4H, Ar), 7.30 (m, 1H, Ar), 7.44 (m, 2H, Ar), 7.65 (d, $J = 8.2$ Hz, 2H, Ar), 7.74 (d, $J = 8.3$ Hz, 2H, Ar). EI-HRMS ($M + H$)⁺ found, 427.2492; calcd for C₂₇H₃₀N₄O, 427.2492.

3-(1*H*-imidazol-1-yl)-*N,N*,2,2-tetramethyl-3-[4-(naphthalen-2-ylamino)phenyl]propanamide (**13**). Compound **13** was prepared from reaction of (**4**) and dimethylamine (2 M in THF) in 61% yield as a brown oil. TLC (97:3 CH₂Cl₂/MeOH, $R_f = 0.59$). ¹H NMR (CDCl₃): δ 1.37 (s, 3H, H-3), 1.41 (s, 3H, H-4), 2.95 (s, 6H, N(CH₃)₂), 5.80 (s, 1H, H-5), 6.23 (s, 1H, NH), 7.08 (m, 4H, Ar), 7.25 (m, 3H, Ar), 7.36 (m, 1H, Ar), 7.41 (m, 1H, Ar), 7.45 (d, $J = 2.6$ Hz, 1H, Ar), 7.66 (d, $J = 7.8$ Hz, 1H, Ar), 7.72 (m, 3H, Ar). ¹³C NMR (CDCl₃): δ 24.34 (CH₃, C-3), 25.16 (CH₃, C-4), 38.75 (2 × CH₃, N(CH₃)₂), 47.93 (C, C-2), 68.69 (CH, C-5), 112.91, 116.91, 120.50, 123.86, 123.92, 126.52, 127.65 (10 × CH), 128.11 (C), 129.24 (CH, imid), 129.51 (C), 129.93 (CH, imid), 129.99 (2 × CH), 134.49, 139.86, 143.67, 175.05 (4 × C). EI-HRMS ($M + H$)⁺ found, 413.2335; calcd for C₂₆H₂₈N₄O, 413.2336.

N,2,2-Trimethyl-3-[4-(naphthalen-2-ylamino)phenyl]-3-(1*H*-1,2,4-triazol-1-yl)propanamide (**19**). This compound was prepared from (**18**) and 33% methylamine in absolute EtOH in 63% yield as a pale yellow oil. TLC (98:2 CH₂Cl₂/MeOH, $R_f = 0.51$). ¹H NMR (CDCl₃): δ 1.33 (s, 6H, H-3, H-4), 2.71 (d, $J = 2.7$ Hz, 3H, NHCH₃), 5.78 (d, $J = 2.8$ Hz, 1H, NHCH₃), 5.87 (s, 1H, NH), 7.08 (d, $J = 7.5$ Hz, 2H, Ar), 7.16–7.19 (m, 1H, Ar), 7.26–7.29 (m, 1H, Ar), 7.37–7.40 (m, 1H, Ar), 7.45–7.50 (m, 3H, Ar), 7.65 (d, $J = 7.6$ Hz, 1H, Ar), 7.74 (d, $J = 7.5$ Hz, 2H, Ar), 7.99 (s, 1H, triaz), 8.19 (s, 1H, triaz). EI-HRMS (M)⁺ found, 400.2133; calcd for C₂₄H₂₅N₅O, 400.2132.

3-(1*H*-imidazol-1-yl)-2,2-dimethyl-3-[4-(naphthalen-2-ylamino)phenyl]propan-1-ol (**15**). A solution of (**14**)²² (0.23 mmol) in dry THF (10 mL) under N₂ was cooled to 0 °C. LiAlH₄ (1 M in THF, 1.2 mmol) was added dropwise, and the reaction mixture was stirred at 0 °C for 1 h and then at room temperature overnight. The reaction was quenched by the addition of EtOAc (70 mL). The organic layer was washed with H₂O (50 mL), dried (MgSO₄), and reduced in vacuo. The residue was purified by flash column chromatography (CH₂Cl₂–MeOH 100:0 v/v increasing to 97:3 v/v) to give the product as a light brown oil in 79% yield. TLC (97:3 CH₂Cl₂/MeOH, $R_f = 0.60$). ¹H NMR (CDCl₃): δ 1.07 (s, 3H, H-3), 1.71 (s, 3H, H-4), 2.48 (s, 1H, OH), 3.26 (d, $J = 8.0$ Hz, 1H, CH₂OH), 3.30 (d, $J = 8.0$ Hz, 1H, CH₂OH), 3.91 (s, 3H, OCH₃), 5.38 (s, 1H, H-5), 5.91 (s, 1H, H-NH), 7.03 (d, $J = 7.8$ Hz, 2H, Ar), 7.11 (m, 3H, Ar), 7.22 (m, 2H, Ar), 7.33 (d, $J = 7.7$ Hz, 2H, Ar), 7.42 (d, $J = 2.8$ Hz, 1H, Ar), 7.57 (d, $J = 8.1$ Hz, 1H, Ar), 7.69 (d, $J = 8.2$ Hz, 1H, Ar), 7.73 (s, 1H, Ar). EI-HRMS (M)⁺ found, 402.2176; calcd for C₂₅H₂₇N₃O₂, 402.2176.

Methyl 2,2-Dimethyl-3-[4-(naphthalen-2-ylamino)phenyl]-3-(1*H*-1,2,4-triazol-1-yl)propanoate (**17**). To a solution of alcohol (**16**)²² (1.5 mmol) in anhydrous CH₃CN (20 mL) were added triazole (6 mmol) and CDT (3 mmol). The mixture was then heated under reflux for 48 h. The reaction mixture was allowed to cool and then extracted with EtOAc (150 mL) and H₂O (3 × 100 mL). The organic layer was dried (MgSO₄), filtered, and reduced in vacuo. The product was purified by flash column chromatography (CH₂Cl₂–MeOH 100:0 v/v increasing to 98:2 v/v) to give the product as a brown oil. Yield, 63%. TLC (99:1 CH₂Cl₂/MeOH, $R_f = 0.57$). ¹H NMR (CDCl₃): δ 1.37 (s, 3H, H-3), 1.40 (s, 3H, H-4), 3.67 (s, 3H, OCH₃), 6.16 (s, 1H, CH), 6.25 (s, 1H, NH), 7.10 (d, $J = 8.7$ Hz, 2H, Ar), 7.25 (dd, $J = 2.3, 8.7$ Hz,

1H, Ar), 7.34 (ddd, $J = 1.1, 7.0, 8.1$ Hz, 1H, Ar), 7.40–7.45 (m, 3H, Ar), 7.49 (d, $J = 2.1$ Hz, 1H, Ar), 7.68 (d, $J = 8.1$ Hz, 1H, Ar), 7.76 (d, $J = 8.8$ Hz, 2H, Ar), 8.00 (s, 1H, H-triaz), 8.14 (s, 1H, triaz). EI-HRMS ($M + Na$)⁺ found, 423.1786; calcd for C₂₄H₂₄N₄O₂Na, 423.1789.

2,2-Dimethyl-3-(4-(naphthalen-2-ylamino)phenyl)-3-(1*H*-1,2,4-triazol-1-yl)propanoic Acid (**18**). To a solution of (**17**) (2 mmol) in THF (5 mL) was added an aqueous solution of LiOH (4 mmol in 5 mL H₂O), and the mixture was homogenized with methanol and heated under gentle reflux for 2 h. The solvent was removed under reduced pressure, H₂O (100 mL) was added, and the unreacted starting materials were extracted with ether (3 × 50 mL). The H₂O layer was acidified with 1 N HCl until pH 3 and extracted with ether (100 mL). The organic layer was dried (MgSO₄), and the solvent was removed under reduced pressure to give the product as a brown oil in 77% yield. TLC (97:3 CH₂Cl₂/MeOH, $R_f = 0.36$). ¹H NMR (CDCl₃): δ 1.23 (s, 3H, H-3), 1.31 (s, 3H, H-4), 5.73 (s, 1H, H-5), 6.27 (s, 1H, NH), 7.13 (d, $J = 7.3$ Hz, 2H, Ar), 7.32–7.42 (m, 6H, Ar), 7.69 (d, $J = 7.4$ Hz, 1H, Ar), 7.76 (d, $J = 7.5$ Hz, 2H, Ar), 8.01 (s, 1H, triaz), 8.22 (s, 1H, COOH), 8.31 (s, 1H, triaz). EI-HRMS ($M + H$)⁺ found, 387.1816; calcd for C₂₃H₂₃N₄O₂, 387.1818.

Molecular Modeling. All molecular modeling studies were performed on a MacPro dual 2.66 GHz Xeon running Ubuntu 9. Ligand structures were built in MOE³³ minimized using the MMFF94x force-field until a rmsd gradient of 0.05 kcal mol⁻¹ Å⁻¹ was reached. Docking simulations were performed using PLANTS³⁴ (aco_ants 20; aco_evap 0.15; aco_sigma 5.0), with ligands docked within the active site of the CYP26A1 homology model,³¹ and the results were visualized in MOE. Molecular dynamics simulations were performed with GROMACS^{35,36} and the Gromos96 force field in a NPT environment. Individual ligand/protein complexes obtained from the docking results were soaked in a triclinic water box and minimized using a steepest descent algorithm to remove unfavorable van der Waals contacts. The system was then equilibrated via a 100 ps MD simulation at 300 K with restrained ligand/protein complex atoms. Finally, a 5 ns simulation was performed at 300 K with a time step of 2 fs and hydrogen atoms constrained with a LINCS algorithm. Visualization of the dynamics trajectories was performed with the VMD software package, version 1.8.3.³⁷

■ ASSOCIATED CONTENT

S Supporting Information. Numbering of compounds for ¹H and ¹³C NMR characterization and ¹³C NMR spectroscopic data for compounds **4–12**, **15**, and **17–19**. This material is available free of charge via the Internet at <http://pubs.acs.org>.

■ AUTHOR INFORMATION

Corresponding Authors

*Tel: +44(0)191-222 5644. Fax: +44(0)191-222 7179. E-mail: j.l.armstrong@newcastle.ac.uk (J.L.A.). Tel: +44(0)2920-876307. Fax: +44(0)2920-874149. E-mail: SimonsC@Cardiff.ac.uk (C.S.).

■ ACKNOWLEDGMENT

We acknowledge Cancer Research UK for funding (M.S.G. and C.E.B., Grant ref. C7735/A9612) and the EPSRC Mass Spectrometry Centre, Swansea, United Kingdom, for mass spectroscopy data.

■ ABBREVIATIONS USED

ATRA, all-*trans*-retinoic acid; RA, retinoic acid; RAMBAs, retinoic acid metabolism blocking agents

REFERENCES

- (1) Gudas, L. J.; Wagner, J. A. Retinoids regulate stem cell differentiation. *J. Cell. Physiol.* **2011**, *226*, 322–330.
- (2) Fields, A. L.; Soprano, D. R.; Soprano, K. J. Retinoids in biological control and cancer. *J. Cell Biochem.* **2007**, *102*, 886–898.
- (3) Orfanos, C. E.; Zouboulis, C. C.; Almond-Roesler, B.; Geilen, C. C. Current use and future potential role of retinoids in dermatology. *Drugs* **1997**, *53*, 358–388.
- (4) Fritsch, P. O. Retinoids in psoriasis and disorders of keratinization. *J. Am. Acad. Dermatol.* **1992**, *27*, S8–S14.
- (5) Thielitz, A.; Krautheim, A.; Gollnick, H. Update in retinoid therapy of acne. *Dermatol. Ther.* **2006**, *19*, 272–279.
- (6) Brecher, A. R.; Orlow, S. J. Oral retinoid therapy for dermatological conditions in children and adolescents. *J. Am. Acad. Dermatol.* **2003**, *49*, 171–182.
- (7) Sanz, M. A. Treatment of acute promyelocytic leukemia. *Hematol. Am. Soc. Hematol. Educ. Program* **2006**, 147–155.
- (8) Imaizumi, M.; Tawa, A.; Hanada, R.; Tsuchida, M.; Tabuchi, K.; Kigasawa, H.; Kobayashi, R.; Morimoto, A.; Nakayama, H.; Hamamoto, K.; Kudo, K.; Yabe, H.; Horibe, K.; Tsuchiya, S.; Tsukimoto, I. Prospective study of a therapeutic regimen with all-*trans* retinoic acid and anthracyclines in combination of cytarabine in children with acute promyelocytic leukaemia: The Japanese childhood acute myeloid leukaemia cooperative study. *Br. J. Haematol.* **2011**, *152*, 89–98.
- (9) Matthay, K. K.; Reynolds, C. P.; Seeger, R. C.; Shimada, H.; Adkins, E. S.; Haas-Kogan, D.; Gerbing, R. B.; London, W. B.; Villablanca, J. G. Long-term results for children with high-risk neuroblastoma treated on a randomized trial of myeloablative therapy followed by 13-*cis*-retinoic acid: A children's oncology group study. *J. Clin. Oncol.* **2009**, *27*, 1007–1013.
- (10) Mills, C. M.; Marks, R. Adverse reactions to oral retinoids. *Drug Saf.* **1993**, *9*, 280–290.
- (11) Collins, M. D.; Mao, G. E. Teratology of retinoids. *Annu. Rev. Pharmacol. Toxicol.* **1999**, *39*, 399–430.
- (12) White, J. A.; Guo, Y.-D.; Baetz, K.; Beckett-Jones, B.; Bonasoro, J.; Hsu, K. E.; Dilworth, F. J.; Jones, G.; Petkovich, M. Identification of the retinoic acid-inducible all-*trans*-retinoic acid 4-hydroxylase. *J. Biol. Chem.* **1996**, *271*, 29922–29927.
- (13) Verfaillie, C. J.; Borgers, M.; van Steensel, M. A. M. Retinoic acid metabolism blocking agents (RAMBAs): A new paradigm in the treatment of hyperkeratotic disorders. *J. Dtsch. Dermatol. Ges.* **2008**, *6*, 355–365.
- (14) Njar, V. C. O.; Gediya, L.; Purushottamachar, P.; Chopra, P.; Vasaitis, T. S.; Khandelwal, A.; Mehta, J.; Huynh, C.; Belosay, A.; Patel, J. Retinoic acid metabolism blocking agents (RAMBAs) for treatment of cancer and dermatological diseases. *Bioorg. Med. Chem.* **2006**, *14*, 4323–4340.
- (15) Verfaillie, C. J.; Vanhoutte, F. P.; Blanchet-Bardon, C.; van Steensel, M. A.; Steijlen, P. M. Oral liarozole vs. acitretin in the treatment of ichthyosis: A phase II/III multicentre, double-blind, randomized, active-controlled study. *Br. J. Dermatol.* **2007**, *156*, 965–973.
- (16) Bryson, H. M.; Wagstaff, A. J. Liarozole. *Drugs Aging* **1996**, *9*, 478484, discussion 485.
- (17) Verfaillie, C. J.; Thissen, C. A.; Bovenschen, H. J.; Mertens, J.; Steijlen, P. M.; van de Kerkhof, P. C. M. Oral R115866 in the treatment of moderate to severe plaque-type psoriasis. *J. Eur. Acad. Dermatol. Venerol.* **2007**, *21*, 1038–1046.
- (18) Verfaillie, C. J.; Coel, M.; Boersma, I. H.; Mertens, J.; Borgers, M.; Roseeuw, D. Oral R115866 in the treatment of moderate to severe facial acne vulgaris: An exploratory study. *Br. J. Dermatol.* **2007**, *157*, 122–126.
- (19) Geria, A. N.; Scheinfeld, N. S. Talarazole, a selective inhibitor of P450-mediated all-*trans* retinoic acid for the treatment of psoriasis and acne. *Curr. Opin. Invest. Drugs* **2008**, *9*, 1228–1237.
- (20) Van Heusden, J.; Van Ginckel, R.; Bruwier, H.; Moelans, P.; Janssen, B.; Floren, W.; van der Leede, B. J.; van Dun, J.; Sanz, G.; Venet, M.; Dillen, L.; Van Hove, C.; Willemsens, G.; Janicot, M.; Wouters, W. Inhibition of all-*trans*-retinoic acid metabolism by R116010 induces antitumour activity. *Br. J. Cancer* **2002**, *86*, 605–611.
- (21) Armstrong, J. L.; Boddy, A. V.; Redfern, C. P. F.; Veal, G. J. Molecular targeting of retinoic acid metabolism in neuroblastoma: the role of the CYP26 inhibitor R116010 in vitro and in vivo. *Br. J. Cancer* **2007**, *96*, 1675–1683.
- (22) Gomaa, M. S.; Bridgens, C. E.; Aboraia, A. S.; Veal, G. J.; Redfern, C. P. F.; Brancale, A.; Armstrong, J. L.; Simons, C. Small molecule inhibitors of retinoic acid 4-hydroxylase (CYP26): Synthesis and biological evaluation of imidazole methyl 3-(4-(aryl-2-ylamino)-phenyl)propanoates. *J. Med. Chem.* **2011**, *54*, 2778–2791.
- (23) Gomaa, M. S.; Armstrong, J. L.; Bobillon, B.; Veal, G. J.; Brancale, A.; Redfern, C. P. F.; Simons, C. Novel azolyl-(phenylmethyl)aryl/heteroarylamines: Potent CYP26 inhibitors and enhancers of all-*trans* retinoic acid activity in neuroblastoma cells. *Bioorg. Med. Chem.* **2008**, *16*, 8301–8313.
- (24) Keyser, J. L.; De Cock, C. J.; Poupaert, J. H.; Dumont, P. A versatile and convenient multigram synthesis of methylidenemalonate diesters. *J. Org. Chem.* **1988**, *53*, 4859–4862.
- (25) Bender, D. M.; Peterson, J. A.; McCarthy, J. R.; Gunaydin, H.; Takano, Y.; Houk, K. N. Cyclopropanecarboxylic acid esters as potential prodrugs with enhanced hydrolytic stability. *Org. Lett.* **2008**, *10*, 509–511.
- (26) Yang, L.; Butora, G.; Jiao, R. X.; Paternak, A.; Zhou, C.; Parsons, W. H.; Mills, S. G.; Vicario, P. P.; Ayala, J. M.; Cascieri, M. A.; Maccoss, M. Discovery of 3-piperidinyl-1-cyclopentanecarboxamide as a novel scaffold for highly potent CC chemokine receptor 2 antagonists. *J. Med. Chem.* **2007**, *50*, 2609–2611.
- (27) Keliher, E. J.; Burrell, R. C.; Chobanian, H. R.; Conkrite, K. L.; Shukla, R.; Baldwin, J. E. Efficient syntheses of four stable-isotope labeled (1R)-menthyl (1S,2S)-(+)-2-phenylcyclopropanecarboxylates. *Org. Biomol. Chem.* **2006**, *4*, 2777–2784.
- (28) Mattsson, S.; Dahlstrom, M.; Karlsson, S. A mild hydrolysis of esters mediated by lithium salts. *Tetrahedron Lett.* **2007**, *48*, 2497–2499.
- (29) Han, I. S.; Choi, J. H. Highly specific cytochrome P450-like enzymes for all-*trans*-retinoic acid in T47D human breast cancer cells. *J. Clin. Endocrinol. Metab.* **1996**, *81*, 2069–2075.
- (30) Riley, R. J.; McGinness, D. F.; Austin, R. P. A unified model for predicting human hepatic, metabolic clearance from in vitro intrinsic clearance data in hepatocytes and microsomes. *Drug Metab. Dispos.* **2005**, *33*, 1304–1311.
- (31) Gomaa, M. S.; Yee, S. W.; Milbourne, C. E.; Barbera, M. C.; Simons, C.; Brancale, A. Homology model of human retinoic acid metabolising enzyme cytochrome P450 26A1 (CYP26A1): Active site architecture and ligand binding. *J. Enzyme Inhib. Med. Chem.* **2006**, *21*, 361–369.
- (32) Perrin, D. D.; Armarengo, W. L. F. *Purification of Laboratory Chemicals*, 3rd ed.; Pergamon Press: New York, 1988.
- (33) Molecular Operating Environment 2008.10 (MOE) Chemical Computing Group Inc Montreal Quebec Canada <http://www.chemcomp.com>.
- (34) Korb, O.; Stütze, T.; Exner, T. E. *Swarm Intell.* **2007**, *1*, 115–134.
- (35) Berendsen, H. J. C.; van der Spoel, D.; van Drunen, R. GROMACS: A message-passing parallel molecular dynamics implementation. *Comput. Phys. Commun.* **1995**, *91*, 43–56.
- (36) Lindahl, E.; Hess, B.; van der Spoel, D. GROMACS 3.0: A package for molecular simulation and trajectory analysis. *J. Mol. Mod.* **2001**, *7*, 306–317.
- (37) Humphrey, W.; Dalke, A.; Schulten, K. VMD—Visual Molecular Dynamics. *J. Mol. Graphics* **1996**, *14*, 33–38.